Prediction of vibration amplitude and surface roughness in boring operation by response surface methodology

B. A. G. Yuvaraju[a,*], B. K. Nanda[a]

[a]*Department of Mechancial Engineering, National Institute of Technology, Rourkela, Odisha-769008, India*

Abstract

Vibrations produced in machine tools like lathe, milling and grinding, etc. during machining operation are one of the primary concern in manufacturing industries. These vibrations not only increase the surface roughness of workpiece but also affect the tool life and noise during the machining operation. In this paper, the effect of input variables viz. speed, feed and depth of cut on output responses such as the vibration amplitude of boring bar and surface roughness of workpiece in boring operation has been studied by providing different composites under the tool using response surface methodology (RSM). The design matrix is created by Box-Behnken design (BBD) with three center points and a single block by three-factors of each three-level to perform the experiments with two different composites such as glass fiber reinforced epoxy (GFRE) and glass fiber reinforced polyester (GFRP). Also, mathematical models have been developed for the output responses as a function of input variables. The developed models have been verified using analysis of variance (ANOVA). Further, the predicted models have been verified by performing the confirmation experiments. It has been found that there is a reduction in surface roughness as well as vibration amplitude with an increase in the number of composite plates placed under the tool.

Keywords: Analysis of Variance (ANOVA); Boring Bar; Box-Behnken design; Composites; Surface roughness (Ra); Response surface methodology; Vibration amplitude;

1. Introduction

Present manufacturing industries are facing difficulties due to vibrations induced in machine tools like lathe, milling, grinding, etc. during machining. Particularly boring on lathe machine is associated with severe vibrations due to long overhang length. Boring is the machining operation in which the pre-drilled holes are enlarged. These induced vibrations are minimized by taking proper care in production planning with assured shape tolerance. Hence, these vibrations have a considerable effect on significant factors such as production cost, productivity, etc. An exhaustive investigation of these vibrations results in a significant step towards solving these problems. The relative motion between the workpiece and tool in cutting direction results deformation of the boring bar as well as cutting insert during the boring operation. A slender and long boring bar is more sensitive to the vibrations induced due to the deformation of material caused by the machining operation. Usually the boring bar is weakest link of the clamping system of the lathe and motion of boring bar may vary with time. The deformation of the workpiece results in the dynamic motion, i.e. vibration. This dynamic motion influences the results of the boring operation, particularly the surface finish of the workpiece. The vibration also influences the tool life.

Bert and Nashif [1, 2] have studied the damping capacity of fiber-reinforced composites to control the vibrations in many applications. They concluded that fiber reinforced composites exhibit more damping capacity compared to metallic structural materials. Lazan [3] has extensively studied the material damping and found that the dynamic stresses are directly related to logarithmic decrement value. Haranath et al. [4] have studied the dynamic analysis of machine tool structures to determine the parameters of damping using viscoelastic layers. They observed that the damping in machine tool structures can be increased by using viscoelastic layers. By considering beam element with applied damping treatment, a theoretical analysis has been presented. Rivin et al. [5] have worked on slender parts

* Corresponding author. Tel.: +91-8338849852;
E-mail address: 515me1002@nitrkl.ac.in

of boring bar and observed an increase in stability of redesigned tool holder using viscoelastic layers with added stiffness and damping. Rahman et al. [6] used various materials to study the structural damping in machine tools and observed that composite material might be a better replacement for the cast iron as it has an excellent stiffness which gives a better surface finish of the product. Miguelez et al. [7] have studied the boring bar behaviour in the presence of passive vibration absorbers using Euler-Bernoulli beam theory for which they considered the first mode of vibration.

Sahoo [8] has studied the influence of input variables on roughness characteristics of the work surface in CNC turning of mild steel. Moreover, developed the model equations for surface roughness and validated by F-Test. It has been observed that an increase in speed and depth of cut results in decrease of surface roughness whereas increase in feed increases surface roughness. Further, the process parameters have been optimized to attain minimum surface roughness using genetic algorithm. Premnath et al. [9] have utilized the RSM technique to develop the predictive models for surface roughness in milling operation. It has been noticed that speed is major significant factor followed by feed rate and weight fraction of Al_2O_3 in composite. Further, it has been observed that predicted and measured values of surface roughness are in good agreement with each other. Bharadwaj et al. [10] have developed predictive models of surface roughness by response surface methodology using rotatable center composite design in turning of steel. It has been noticed that feed is the major significant parameter whereas the depth of cut has no significance. Kant et al. [11] have developed predictive models to minimize the surface roughness as well as power consumption. It has been noticed that feed is the major significant parameter followed by the depth of cut and speed. Mahesh et al. [12] have developed predicted models of surface roughness in terms of milling parameters using the genetic algorithm. The minimum predicted value obtained for surface roughness by GA is about 0.25 um. The measured and predicted values are in good agreement. Rao and Murthy [13] have developed predictive model equations of surface roughness and tool vibration in boring operation using statistical methods such as RSM, ANN. It has been noticed that ANN is much better than RSM models in the response model prediction. Further, the machining parameters are optimized to achieve the minimum tool vibration and surface roughness multi-optimization technique.

Nomenclature

S	Speed, rpm
F	Feed, mm/rev
D	Depth of cut, mm
Ra	Surface roughness, µm
A	Vibration amplitude, mV
y	Output response
β_0 , β_i , and β_{ij}	Regression coefficients, where i=1,2…n and j=1,2,…n
x_1, $x_2 \ldots x_n$	Input variables
$\in$	Random error

2. Experimental details

The experiments are carried out in ROCIO 180X750 conventional lathe machine, which is equipped with spindle and coolant motors of capacity 4 kW and 0.06 kW respectively. Boring bar (A16R-SCLCR-09) of diameter 16 mm with carbide inserts (CCMT-09T308-MU-TN2000) are used to perform the boring operation. To perform each experiment a new cutting insert and cutting length of 30 mm are used. Further, the surface roughness (Ra) is measured using Taylor-Hobson Talysurf tester. Figs. 1a and 1b represent the cutting insert and boring bar utilized in the experiment respectively. No cutting fluid is used to perform the experiments.

Fig. 1. (a) Cutting tool insert (CCMT-09T308-MU-TN2000); (b) Boring bar (A16R-SCLCR-09).

The design matrix is created with Box-Behnken design (BBD) by considering three-factors of each three-level to perform experiments using statistica software. The DOE created by BBD contains a set of 15 experiments with three center points and a single block. Different levels of input factors used in boring operation are presented in Table-1.

Table 1. Allocation of various levels to the process parameters

Input factor	Units	Level-1	Level-2	Level-3
Spindle Speed	rpm	92	140	220
Feed rate, F	mm/rev	0.1	0.2	0.3
Depth of cut	mm	0.1	0.2	0.3

2.1. Setup and procedure

The experimental setup mainly consists of a lathe, boring bar, cutting inserts, workpiece, composite plates, accelerometer and digital storage oscilloscope. Fig. 2 represents the schematic diagram of experimental setup.

Initially, the boring bar with carbide insert is fixed on the tool post of conventional centre lathe and mild steel workpiece is mounted on the headstock. A contact type accelerometer is placed on the boring bar in the cutting speed direction, which is used to measure the vibration signals induced during machining. After that, the boring operation is performed on the lathe with various controlling parameters and the vibrations induced in the boring bar in cutting speed direction are recorded on the oscilloscope and analysed. The root mean square of the vibration amplitudes of vibration signal recorded by oscilloscope is noted down for analysis. Further, the surface roughness of workpiece is measured using Talysurf. The average of three set of readings is taken for surface roughness. Response surface methodology (RSM) is employed to develop the model equations for the responses i.e. vibration amplitude of the boring bar and surface roughness of machined part as a function of input variables. The experiments are repeated for one and two layers of different composites, i.e. Glass Fiber Reinforced Epoxy (GFRE) and Glass Fiber Reinforced Polyester (GFRP) placed on the tool post. Finally, the predicted and experimental models are verified by performing the confirmation experiments for optimum values of input parameters.

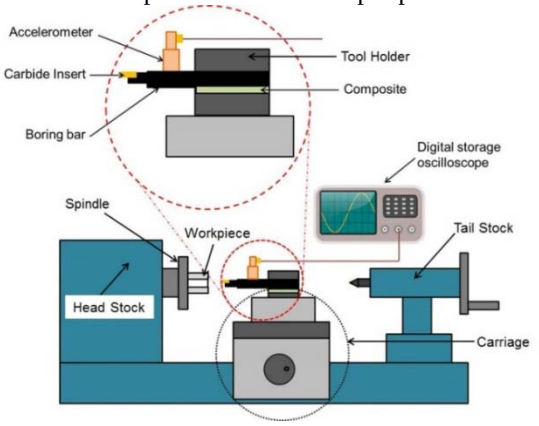

Fig. 2. Schematic diagram of experimental setup.

3. Mathematical models for surface roughness and vibration amplitude

3.1. Experimental design matrix

A three-level three-factor Box-Behnken Design (BBD) is utilized to perform the experiments, which contains a set of 15 experiments with three center points and a single block. The linear, quadratic and interaction effects of input variables on the vibration amplitude and surface roughness are estimated. The experiments are performed in the order given by design matrix obtained by the statistica software. Table-2 represents the results obtained from experiments for vibration amplitude as well as surface roughness.

3.2. Mathematical models

Response surface methodology (RSM) gives the relationship between measured outputs and process parameters. In all the five cases, a nonlinear relationship between output responses and input parameters. The mathematical expression representing the surface of response for input parameters is given in Eq. (1).

$$y = \beta_0 + \sum_{i=1}^{n} \beta_i x_i + \sum_{i=1}^{n} \beta_{ii} x_i^2 + \sum\sum_{i<j} \beta_{ij} x_i x_j + \in \quad (1)$$

The method applied to estimate the regression coefficients by solving the response model of second order is method of least squares. Further, the fitted response surface is analysed using response surface analysis. The method of least square is employed to fit the model equation containing process parameters to minimize the residual errors by deviations obtained from sum of squares between the estimated and actual responses. This method involves the calculation of the regression coefficients [14]. These coefficients in Eq. (1) are determined by RSM using Statistical software, i.e., Statistica V10. The mathematical models are developed for vibration amplitude and surface roughness in coded values, presented in Table-3.

Table 2. Experimental results for vibration amplitude and surface roughness.

Speed (rpm)	Feed (mm/rev)	Depth of cut (mm)	Without any composite		With one GFRE plate		With two GFRE plates		With one GFRP plate		With two GFRP plates	
			A (mV)	Ra (µm)	A (mV)	Ra (µm)	A (mV)	Ra (µm)	A (mV)	Ra (µm)	A (mV)	Ra (µm)
140	0.1	0.1	140.64	6.1	194.07	5.93	133.51	5.54	90.99	5.67	89.85	5.13
220	0.3	0.2	252.63	12.5	248.04	12.57	227.15	12.07	247.17	9.93	167.18	11.13
220	0.2	0.1	206.89	11.02	319.77	11.1	234.85	9.03	287.58	9.6	166.5	7.87
140	0.3	0.1	144.18	11.83	219.02	10.5	144.95	10.03	97.16	9.8	122.16	8.67
220	0.1	0.2	199.13	8.93	230.72	10.23	334.86	5.03	257.72	6.87	211.74	5.1
92	0.1	0.2	121.74	5.83	62.48	5.6	162.8	8.57	86.84	5.67	47.06	7.6
92	0.2	0.1	109.14	10.03	110.45	9.33	71.71	7.83	102.94	4.87	59.17	8.87
140	0.2	0.2	238.42	12.47	187.79	11.01	169.41	12.2	195.83	11.07	128.61	11.47
140	0.1	0.3	241.07	12.03	145.57	6.4	236.22	9.03	205.24	6.2	176.95	7.6
140	0.3	0.3	243.85	13.67	286.1	10.01	180.61	11.87	152.67	12.8	153.2	11.47
220	0.2	0.3	239.94	14.1	270.98	12.87	248.04	11.47	373.53	10.87	277.65	10.2
140	0.2	0.2	239.99	13.03	201.49	9.52	176.75	10.87	158.19	9.2	140.06	9.33
140	0.2	0.2	265.54	11.8	187.69	8.1	176.75	9.2	188.9	10.67	120.95	10.8
92	0.3	0.2	156.98	13.01	111.39	9.8	129.95	11.27	125.7	11.87	101.57	11.2
92	0.2	0.3	190.012	12.33	129.42	8.53	129.92	11.93	96.73	9.73	86.01	9.17

Table 3. surface roughness and vibration amplitude models predicted by RSM using various composites.

Type of composite used	Predicted mathematical models by RSM
Without any composite	Ra = -12.73 + 0.0810 S + 122.0 F + 22.6 D - 0.000201 S*S - 170.6 F*F + 29.4 D*D - 0.057 S*F + 0.018 S*D - 110.0 F*D
	Amp = -485 + 4.565 S + 1151 F + 1758 D - 0.01189 S*S - 2971 F*F - 2584 D*D + 1.08 S*F - 2.22 S*D - 19 F*D
GFRE with one plate	Ra = 7.6 - 0.011 S + 28.5 F - 14.0 D + 0.000021 S*S - 82 F*F - 47 D*D + 0.019 S*F + 0.117 S*D + 62 F*D
	Amp = -214 + 5.167 S + 471 F - 1445 D - 0.00959 S*S - 1282 F*F + 3168 D*D - 1.67 S*F - 2.80 S*D + 2890 F*D
GFRE with two plates	Ra = 11.9 - 0.2116 S + 129.7 F + 27.1 D + 0.000598 S*S - 316.1 F*F - 66.1 D*D - 0.061 S*F + 0.006 S*D + 90.0 F*D
	Amp = -180 - 0.05 S + 2102 F + 324 D + 0.00390 S*S - 4015 F*F - 431 D*D - 1.52 S*F + 3.06 S*D - 1468 F*D
GFRP with one plate	Ra = 5.8 - 0.1058 S + 54.6 D + 44.8 F + 0.000078 S*S - 100.0 D*D - 230.0 F*F - 0.015 S*D + 0.432 S*F + 20.0 D*F
	Amp = -201.6 + 2.045 S + 1758 D - 250 F + 0.00030 S*S - 2152 D*D + 2104 F*F - 2.02 S*D - 3.29 S*F - 1676 D*F
GFRP with two plates	Ra = 1.8 - 0.0611 S + 52.2 F + 63.1 D + 0.000190 S*S - 202.5 F*F -95.8 D*D + 0.119 S*F - 0.181 S*D + 133.9 F*D
	Amp = -190.9 + 1.908 S + 1053 F - 308 D - 0.00251 S*S - 489 F*F + 1056 D*D - 3.75 S*F + 3.29 S*D - 1401 F*D

4. Results and discussions

It is observed that the models predicted for GFRE composite with two plates give better vibration amplitude and surface roughness compared to other models. The results obtained by GFRE composite with two plates are discussed below.

4.1. Analysis of variance

The effect of input parameters on selected responses (such as vibration amplitude and surface roughness) are evaluated for boring operation without and with composites on the tool post during the boring operation. A quadratic empirical relationship is developed between controllable parameters and responses. Analysis of variance (ANOVA) is carried out for second order model to check the fitness. The results obtained for GFRE composite with two plates are presented below.

Table 4. ANOVA for surface roughness when using GFRE with two plates.

Source	Df	Adj SS	Adj MS	F-value	P-Value
Model	9	141.286	15.6984	5.08	0.044
S	1	42.320	42.320	13.70	0.014<0.05
F	1	10.743	10.743	3.48	0.121
D	1	29.924	29.924	9.69	0.026<0.05
S*S	1	18.939	18.939	6.13	0.056
F*F	1	36.896	36.896	11.95	0.018<0.05
D*D	1	1.614	1.614	0.52	0.502
S*F	1	0.627	0.627	0.20	0.671
S*D	1	0.006	0.006	0.00	0.966
F*D	1	3.240	3.240	1.05	0.353
Error	5	15.442	3.0884		
Total	14	156.728			

The analysis of variance for surface roughness and vibration amplitude using two GFRE composite plates under the tool is presented in Tables 4 and 5 respectively. It has been noticed that depth of cut as well as speed are the linear variables that are significant, whereas feed is only the quadratic parameter that is significant at a confidence level of 0.05.

Table 5. ANOVA for vibration amplitude when using GFRE with two plates.

Source	Df	Adj SS	Adj MS	F-value	P-Value
Model	9	94137	10459.7	7.64	0.019
S	1	71024.9	71024.9	51.88	0.001<0.05
F	1	93.8	93.8	0.07	0.804
D	1	8786.5	8786.5	6.42	0.05=0.05
S*S	1	804.9	804.9	0.59	0.478
F*F	1	5951.5	5951.5	4.35	0.091
D*D	1	68.6	68.6	0.05	0.832
S*F	1	389.3	389.3	0.28	0.617
S*D	1	1586.9	1586.9	1.16	0.331
F*D	1	862.6	862.6	0.63	0.463
Error	5	6845	1368.9		
Total	14	100982			

4.2. Effect of input variables on surface roughness

The main effects plot of surface roughness with input variables is shown in Fig. 3. It is observed that an increase in speed decreases the surface roughness. The tendency to form the Built-up edge at higher speed is reduced due to the amount of heat carried away by the chip is more whereas heat dissipated to the workpiece is less, this results in a decrease of surface roughness value. It is noticed that the maximum surface roughness attained at a high-level speed, i.e., 220 rpm.

Moreover, it is found that there is an increase in surface roughness with an increase in feed till 0.2 mm/rev, further increase in feed decreases the surface roughness. Thus, the optimum surface roughness is attained at a low-level feed, i.e., 0.1 mm/rev. If the feed increases then the contact area between tool and workpiece increases, this results in an increase of cutting forces on the tool. It gives higher surface roughness of the machined surface.

Further, it is noticed that increase in depth of cut will increase the surface roughness. The material removal rate and cross-sectional area of chip increase with an increase in depth of cut, it is because of increase in cutting force on the tool. Therefore, the chatter also increases that results in higher surface roughness. Thus, the optimum surface roughness is attained a low-level depth of cut, i.e., 0.1 mm.

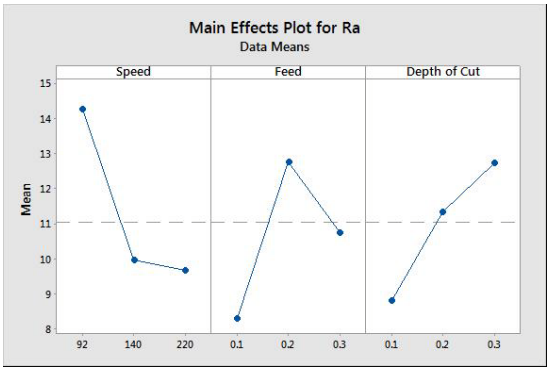

Fig. 3. Main effects plot for surface roughness.

4.3. Effect of input variables on vibration amplitude

Fig. 4 represents the main effects plot for vibration amplitude. It is observed that the vibration amplitude increases with an increase in depth of cut as well as speed. In addition, it is noticed that the vibration amplitude increases till 0.2 mm/rev feed and then it decreases. The increase in speed as well as the depth of cut results in an increase of cutting forces on the tool, which produces more chatter resulting higher vibration amplitude. The optimum conditions of speed, feed and depth of cut for GFRE with two plates attain minimum vibration amplitude at 92 rpm, 0.3 mm/rev and 0.1 mm respectively.

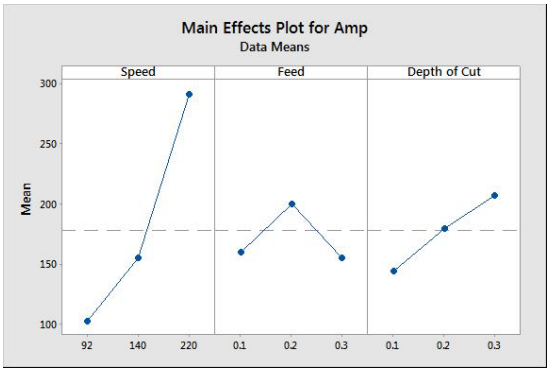

Fig. 4. Main effects plot for vibration amplitude.

4.4. Effect of speed-feed interaction on surface roughness and vibration amplitude

Figs. 5a and 5b represent the surface plots for the surface roughness and vibration amplitude respectively at a constant depth of cut of 0.2 mm. It is noticed that there is a decrease in surface roughness with increase in the speed from 92 to 140 rpm and further it increases with increase in speed till 220 rpm for all the levels of feed. The trend of decreasing surface roughness for three levels of feed is not changed. Thus, this interaction effect is less significant.

It is found that the maximum surface roughness of 16.15 µm attained at a feed and speed of 0.2 mm/rev and 92 rpm respectively, whereas it attains a minimum of 7.69 µm at a feed and speed of 0.1 mm/rev and 140 rpm respectively. The optimum surface roughness is obtained at high-level speed with low-level feed combination. Further, it is noticed that the vibration amplitude attains a maximum of 314.16 mV at a feed and speed of 0.2 mm/rev and 220 rpm respectively, whereas it attains a minimum of 91.49 mV at a feed and speed of 0.3 mm/rev and 92 rpm respectively. The optimum vibration amplitude is obtained at low-level speed with high-level feed combination.

a

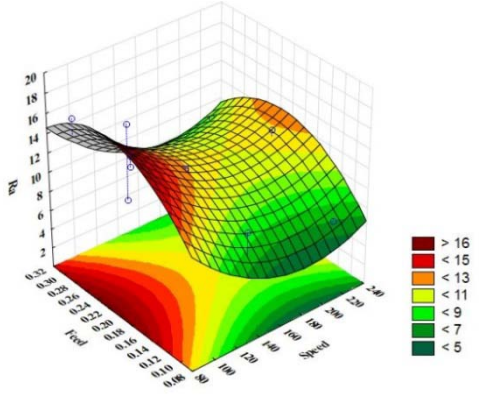

b

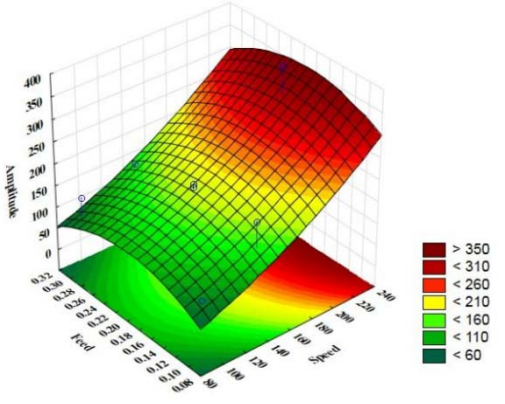

Fig. 5. Surface plot at a depth of cut of 0.2 mm a) for surface roughness; b) for vibration amplitude.

4.5. Effect of speed-depth of cut interaction on surface roughness and vibration amplitude

Figs. 6a and 6b represent the surface plots for the surface roughness and vibration amplitude respectively at a constant feed of 0.2 mm/rev. It is noticed that there is a decrease in surface roughness with increase in the speed from 92 to 140 rpm and further it increases with increase in speed till 220 rpm for all the levels of depth of cut. The trend of decreasing surface roughness value for all three levels of depth of cut is not changed. Thus, this interaction effect is less significant.

a b

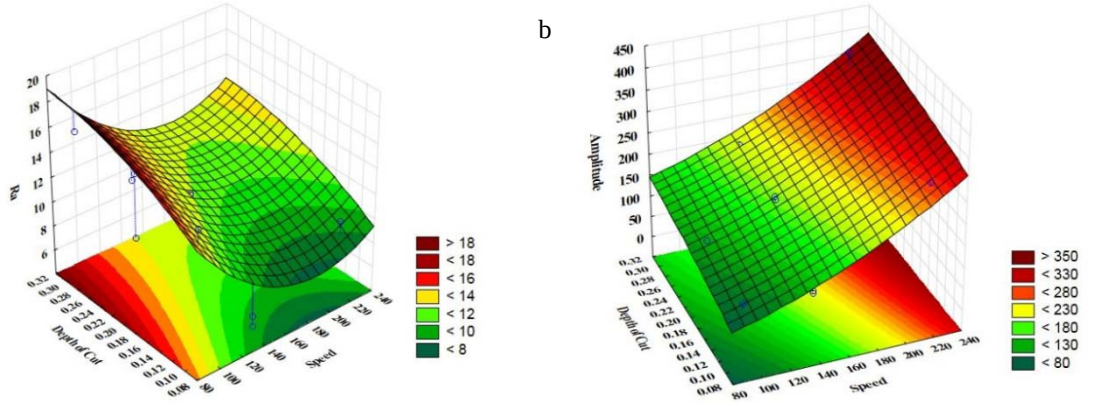

Fig. 6. Surface plot at a feed of 0.2 mm/rev a) for surface roughness; b) for vibration amplitude.

It is found that the maximum surface roughness of 17.41 μm attained at a speed and depth of cut of 92 rpm and 0.3 mm respectively, whereas it attains a minimum of 9.52 μm at a speed and depth of cut of 140 rpm and 0.1 mm respectively. The optimum surface roughness is obtained at low-level depth of cut with high-level speed combination.

Further, it is observed that the vibration amplitude attains a maximum of 362.97 mV at a speed of 220 rpm and depth of cut of 0.3 mm, whereas it attains a minimum of 107.12 mV at a speed and depth of cut of 92 rpm and 0.1 mm respectively. The optimum vibration amplitude is attained at low-level depth of cut with low-level speed combination.

4.6. Effect of feed-depth of cut interaction on surface roughness and vibration amplitude

Figs. 7a and 7b represent the surface plots for the surface roughness and vibration amplitude respectively at a constant speed of 140 rpm. It is noticed that there is an increase in surface roughness with increase in the feed from 0.1 to 0.2 mm/rev and further it decreases with increase in feed till 0.3 mm/rev for all the levels of depth of cut. The trend of increasing surface roughness is not changed for all the levels of depth of cut. Thus, this interaction effect is less significant.

a b

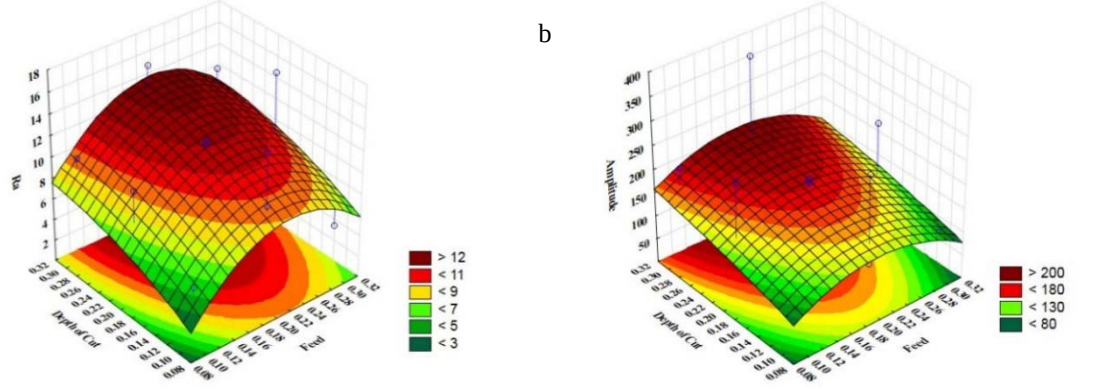

Fig. 7. Surface plot at a speed of 140 rpm a) for surface roughness; b) for vibration amplitude.

It is found that the maximum surface roughness of 13.42 μm attained at a depth of cut and feed of 0.3 mm and 0.2 mm/rev respectively, whereas it attains a minimum of 5.98 μm at a depth of cut and feed of 0.1 mm and 0.1 mm/rev respectively. The optimum surface roughness is attained at low-level depth of cut with low-level feed combination.

Further, it is noticed that the vibration amplitude attains a maximum of 205.53 mV at a depth of cut and feed of 0.3 mm and 0.2 mm/rev respectively, whereas it attains a minimum of 94.46 mV at a depth of cut and feed of 0.1 mm and 0.1 mm/rev respectively. The optimum vibration amplitude is achieved at of low-level depth of cut with low-level feed combination.

4.7. Optimal cutting conditions

It is observed that the optimum condition for surface roughness for GFRE composite with two plates is obtained with combination of speed, feed and depth of cut of 220 rpm, 0.1 mm/rev and 0.1mm respectively. Further, it is observed that the optimum condition for vibration amplitude for GFRE composite with two plates is obtained at a speed, feed and depth of cut of 92 rpm, 0.3 mm/rev and 0.1mm respectively.

4.8. Confirmation tests

The predicted models are verified and validated by performing the confirmation experiments for optimum conditions of input parameters. The experimental results are validated with corresponding predicted models and presented in Table 6. The predicted and experimental values of surface roughness as well as vibration amplitude are compared. In addition, the percentage errors for various composites are computed and observed that the percentage error is within the range of -3 to 3% for surface roughness and -6 to 7% for vibration amplitude. Hence, the response equations developed from RSM for vibration amplitude and the surface roughness are authentic.

Table 6. Confirmation test results for various composites.

Process Parameter Composite type		Speed (rpm)	Feed (mm/rev)	Depth of cut (mm)	Predicted	Experimental	% Error
Without any composite	Ra	92	0.1	0.1	4.89	4.97	1.61
	A	92	0.1	0.1	59.02	62.93	6.21
With one GFRE plate	Ra	92	0.1	0.3	5.63	5.75	2.09
	A	92	0.1	0.2	43.11	45.34	4.92
With two GFRE plates	Ra	140	0.1	0.1	5.98	5.84	-2.40
	A	92	0.3	0.1	46.04	43.93	-4.80
With one GFRP plate	Ra	140	0.1	0.1	5.19	5.37	3.35
	A	92	0.3	0.1	98.05	105.38	6.96
With two GFRP plates	Ra	140	0.1	0.1	5.99	5.83	-2.74
	A	92	0.1	0.1	25.32	23.97	-5.63

5. Conclusions

The effect of input variables viz. speed, feed and depth of cut on outputs such as vibration amplitude and surface roughness in boring operation has been studied by response surface methodology. Further, the models for output responses have been developed. Based on this the following conclusions are drawn:

- Speed and depth of cut are linear input factors that are significant, whereas feed is only the quadratic parameter that is significant for both surface roughness and vibration amplitude.
- For GFRE composite with two plates, the optimum surface roughness is attained at a speed, feed and depth cut of 220 rpm, 0.1 mm/rev and 0.1 mm respectively, whereas the optimum vibration amplitude is attained at a speed, feed and depth cut of 92 rpm, 0.3 mm/rev and 0.1 mm respectively, from main effects plot.
- The experimental results are validated using the predicted models of vibration amplitude and surface roughness by performing the confirmation experiments and the percentage error has been computed. The range of percentage error for surface roughness and vibration amplitude are -3 to 3% and -6 to 7% respectively.

References

[1] C.W. Bert, Composite materials: A survey or the damping capacity of fiber-reinforced composites, 1980.

[2] A.D. Nashif, D.I.G. Jones, and J.P. Henderson, Vibration Damping, A wiley-interscience publication, 1985.

[3] B.J. Lazan, Damping of materials and members in structural mechanics, Pergamon Press Ltd, Oxford, England, 1968.

[4] S. Haranath, N. Ganesan, and B.V.A. Rao, Dynamic analysis of machine tool structureswith applied damping treatment, Int. J. Mach. Tools Manuf., 27:1 (1987) 43–55.

[5] E.I. Rivin, and H. Kang, Improvement of machining conditions for slender parts by tuned dynamic stiffness of tool, Int. J. Mach. Tools Manuf., 29:3 (1989) 361–376.

[6] M. Rahman, A. Mansur, and B. Karim, Non-conventional Materials for Machine Tool Structures, JSME Int. J. Ser. C Mech. Syst. Mach. Elem. Manuf., 44:1 (2001) 1–11.

[7] M.H. Miguelez, L. Rubio, J.A. Loya, and J. Fernández-Sáez, Improvement of chatter stability in boring operations with passive vibration absorbers, Int. J. Mech. Sci., 52:10 (2010) 1376–1384.

[8] A.A. Premnath, T. Alwarsamy, T. Abhinav, and C.A. Krishnakant, Surface roughness prediction by response surface methodology in milling of hybrid aluminium composites, ICMOC, Procedia Engineering, 38 (2012) 745-752.

[9] P. Sahoo, Optimization of turning parameters for surface roughness using RSM and GA, Advances in Production Engineering & Management, 6:3 (2011) 197-208.

[10] Bhuvnesh Bhardwaj, Rajesh Kumar and Pradeep K Singh, Surface roughness (Ra) prediction model for turning of AISI 1019 steel using response surface methodology and Box–Cox transformation, Proc IMechE Part B: J Engineering Manufacture 228(2) (2013) 223–232.

[11] G. Kant, K. S. Sangwan, Prediction and optimization of machining parameters for minimizing power consumption and surface roughness in machining, Journal of Cleaner Production, 83 (2014) 151-164.

[12] G. Mahesh, S. Muthu and S. R. Devadasan, Prediction of surface roughness of end milling operation using genetic algorithm, Int J Adv Manuf Technol, 77 (2015) 369–381.

[13] K. V. Rao and P. B. G. S. N. Murthy, Modeling and optimization of tool vibration and surface roughness in boring of steel using RSM, ANN and SVM, Journal of intelligent manufacturing, (2016) 1-11.

[14] S. D. Philip, P. Chandramohan, and P.K. Rajesh, Prediction of surface roughness in end milling operation of duplex stainless steel using response surface methodology, Journal of engineering science and technology, 10:3 (2016) 330-352.